

Soft Matter

Accepted Manuscript



This is an *Accepted Manuscript*, which has been through the Royal Society of Chemistry peer review process and has been accepted for publication.

Accepted Manuscripts are published online shortly after acceptance, before technical editing, formatting and proof reading. Using this free service, authors can make their results available to the community, in citable form, before we publish the edited article. We will replace this *Accepted Manuscript* with the edited and formatted *Advance Article* as soon as it is available.

You can find more information about *Accepted Manuscripts* in the [Information for Authors](#).

Please note that technical editing may introduce minor changes to the text and/or graphics, which may alter content. The journal's standard [Terms & Conditions](#) and the [Ethical guidelines](#) still apply. In no event shall the Royal Society of Chemistry be held responsible for any errors or omissions in this *Accepted Manuscript* or any consequences arising from the use of any information it contains.

ARTICLE

Effect of interaction heterogeneity on colloidal arrangements at a curved oil-water interface

Cite this: DOI: 10.1039/x0xx00000x

Mina Lee^a, Daeyeon Lee^b, and Bum Jun Park^{a*}Received 00th xxx xxx,
Accepted 00th xxx xxx

DOI: 10.1039/x0xx00000x

www.rsc.org/

We report the unique arrangement behaviour of colloidal particles at a curved oil-water interface. Particles trapped at a centrosymmetrically curved oil-water interface, formed by placing an oil lens at a neat air-water interface, organize into diverse arrangement structures due to electrostatic repulsion under the gravitational field. To reveal a possible mechanism behind the observed diversity, we investigate the interactions between pairs of particles at the curved oil-water interface. The magnitude of electrostatic repulsive interactions between pairs of particles is determined by minimizing the total potential of the particle pairs. We show that the pair interactions are quite heterogeneous, following a Gamma distribution. By using the experimentally determined pair potential and the heterogeneity in the potential as input parameters for Monte Carlo simulations, we show that such interaction heterogeneity affects the particle arrangements at the curved interface and results in the observed diversity in the particle arrangement structures. We believe that this work prompts further experimental and simulation studies to extensively understand hierarchical relations from small scale measurements (e.g., pair interactions, heterogeneity) to bulk scale properties (e.g., microstructure, interfacial rheology).

Introduction

Colloidal particles attach irreversibly to fluid-fluid interfaces to reduce the area between two immiscible fluids.^{1,2} Such adsorption behaviour enables conventional colloids to be used as solid surfactants, which can serve as alternatives for molecular surfactants that may be expensive or environmentally hazardous.¹⁻⁴ When colloidal particles are trapped at fluid-fluid interfaces, two types of lateral interactions between the particles play critical roles in determining their behaviour: electrostatic and capillary interactions.⁵⁻⁹ While electrostatic interactions, which stem from the local charge dissociation in polar or apolar fluid phases, result in repulsion,⁹⁻¹⁴ capillarity due to the chemical and geometrical anisotropy of particles typically leads to particle attraction at the fluid-fluid interface.^{5,6, 12, 15-24} Although significant efforts have been devoted to understanding the behaviour of particle assemblies and arrangements at fluid-fluid interfaces, the majority of these studies focus on planar fluid-fluid interfaces.^{18, 22, 24-27} However, considering that the practical applications of colloids as solid surfactants typically involve curved interfaces such as emulsion droplets, bubbles, and multiphase fluid streams, it is critical that the behaviour of particles at curved interfaces, influenced by the surface curvature and confinement, be investigated and understood.

Recent studies focusing on the interactions of particles on non-planar surfaces have revealed the importance of surface

curvature and its critical impact on the particle interaction and assembly at curved interfaces.^{21, 28-31} Previous reports, for example, have demonstrated that particles undergo deterministic assembly driven by capillary attraction to lower the free energy of the system on curved interfaces.²⁸ Thus, investigating the role of electrostatic interactions between particles and non-deterministic assembly behaviour at curved fluid interfaces is critical in deepening our understanding of colloidal behaviour at fluid interfaces. In this work, we study unique arrangement behaviours of multiple particles at a centrosymmetrically curved oil-water interface. We show that particles organize into diverse structures owing to the heterogeneity of pair interactions. We develop a novel method to measure the pair interactions at the curved interface and the heterogeneity of the interactions. The effect of interaction heterogeneity on the arrangement behaviours at the curved interface is further investigated using Monte Carlo (MC) simulations that use experimentally determined pair interactions.

Materials and Method

A concave oil-water interface is generated by gently placing a small amount of hydrocarbon oil (i.e., *n*-decane) on water (resistivity > 18.2 MΩ·cm), forming an oil lens on the water surface. Polystyrene particles (PS) with $2R \approx 200 \mu\text{m}$ in diameter are prepared by using microfluidics and are

individually placed outside the oil lens at the air-water interface using a micropipette.³² After introducing the particles, the sample cell is covered to minimize evaporation and convection. The particles residing initially at the air-water interface spontaneously transport through the triple phase boundary and move to the center of the oil lens while being trapped at the oil-water interface. Such particle transport phenomena are driven by the radial gradient in the attachment energy of particles to different fluid interfaces (air-water, air-oil, and oil-water interfaces) and gravity.³² Notably, although the particles tend to collect around the bottom of the curved oil-water interface due to gravity, the Bond number, which is the ratio of gravitational force to the interfacial tension force, is sufficiently small ($Bo \approx 10^{-3}$), and thus local interface deformation around each particle due to gravity is unlikely to occur. Microscopic snapshots are captured using a CCD camera (Hitachi KP-M1AN) to determine the equilibrium separation between particles as well as the arrangement structures of multiple particles.

Results and Discussion

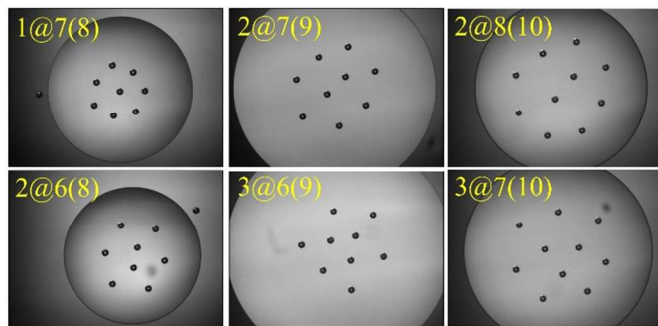


Fig. 1 Arrangement of multiple particles at the curved oil-water interface. The arrangement structure composed of eight, nine, and ten particles exhibit two distinct patterns. “x@y” indicates that “x” inner particles are surrounded by “y” outer particles. The number in parentheses is the total number of particles (x + y). The scale bar is 1 mm.

Interestingly, we find that particles at the curved oil-water interface organize into distinctively different arrangement structures. For instance, the arrangements composed of eight, nine, and ten particles exhibit two different structures in each case, as shown in Fig. 1. Eight particles adopt one-inside (1@7) or two-inside (2@6) configurations, whereas nine and ten particles form either two-inside (2@7 and 2@8) or three-inside (3@6 and 3@7) structures. It is evident that the number of inner particles is determined in a way that the number of its neighbouring particles is between five and seven. Note that these configurations do not depend on the amount of oil that is used to form the oil lens. To understand this unique arrangement behaviour, we develop a novel method to determine the interaction magnitude between two particles at the curved oil-water interface. Subsequently, we use MC simulations employing experimentally determined pair

interactions to compare the simulation results to the experimental arrangement structures.

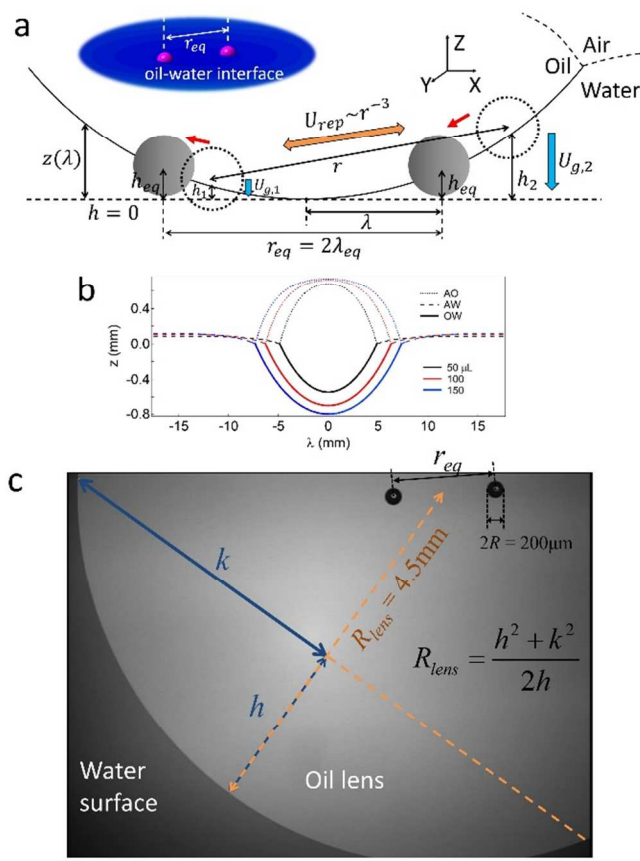


Fig. 2 Measurements of the pair interaction magnitude at the curved oil-water interface. (a) Schematic of two particles at the curved interface that migrate to their equilibrium positions. (b) Shape of oil lens on a water surface, depending on the amount of oil (spreading coefficient, $S = -3.72$). (c) An example snapshot shows two particles with $2R \approx 200 \mu\text{m}$ at the curved oil-water interface. The scale bar is 1 mm.

To determine the magnitude of the interaction between a pair of particles, two particles are placed at the curved oil-water interface. The shape of the oil lens (air-water, air-oil, and oil-water interfaces) in Fig. 2 is determined by using a previously reported method in which the spreading coefficient of *n*-decane is $S_{oil} = -3.72$.^{32, 33} Electrostatic-induced particle repulsion is represented by

$$\frac{U_{rep}}{k_B T} = ar^{-3} \quad (1)$$

where a indicates the magnitude of the repulsive pair interaction, k_B is the Boltzmann's constant, T is the temperature, and r is the center-to-center separation between the two particles.^{9, 10, 12, 14, 15} Notably, it has been measured that the electrostatic repulsions at a fluid-fluid interface (e.g., an oil-water interface) are abnormally strong, compared to that of the electrostatic double layer interactions in a single fluid medium (e.g., water). Such strong electrostatic repulsions at the interface can be attributed to the dipole-dipole repulsion in

which an asymmetric counterion distribution around each particle creates the dipole perpendicular to the interface.^{7-9, 14} The electrostatic repulsions at the interface may be also due to surface residual charges in the oil phase that can be dissociated and stabilized by a small amount of water captured in cavities of the particle surface.^{10, 25} Although the exact mechanism of the electrostatic interactions at the interface is not fully understood yet, the experimental and theoretical studies of the scaling exponent consistently demonstrate the scaling behaviour of $U_{rep} \sim r^{-3}$. The curvature radius of the oil-water interface is sufficiently large compared to the particle size, and therefore, the scaling behaviour of the repulsive interaction, i.e., $U_{rep} \sim r^{-3} \sim \lambda^{-3}$, reasonably captures the particle interactions on such curved interfaces. In this case, λ is the radial distance from the center of the concave interface. The particles at the curved oil-water interface tend to collect at the bottom of the curved interface due to gravity. The corresponding potential energy for two particles under the gravitational field is given by¹

$$U_{grav} = g(\rho_p V_p - \rho_w V_{pw} - \rho_o V_{po})(h_1(\lambda) + h_2(\lambda)) \quad (2)$$

where V_p is the volume of particle, ρ is the density, g is the gravitational acceleration, and h_1 and h_2 are the vertical distances of the two particles from the bottom of the oil lens (Fig. 2a). The subscripts p , w , o denote the particle, water, and oil, respectively. Using geometric relations, the particle volumes immersed in each fluid phase are

$$V_{pw} = \frac{\pi R^3}{3} (2 + 3 \cos \theta_c - \cos^3 \theta_c) \quad (\text{in water})$$

$$V_{po} = \frac{\pi R^3}{3} (2 - 3 \cos \theta_c + \cos^3 \theta_c) \quad (\text{in oil})$$

where $\theta_c = 105^\circ$ is the three-phase contact angle of the particle at the oil-water interface measured using the gel trapping method.^{32, 34} The interface height, $h(\lambda)$, where a particle resides, is obtained by interpolation of $z(\lambda)$ at a given value of λ (Fig. 2b). When the electrostatic repulsion and the gravitational energy of the two particles come to an equilibrium, the particles rest at an equilibrium height ($h_{eq}(\lambda) = h_1(\lambda) = h_2(\lambda)$) with an equilibrium separation ($r_{eq} = 2\lambda_{eq}$) (Fig. 2a and 2c).

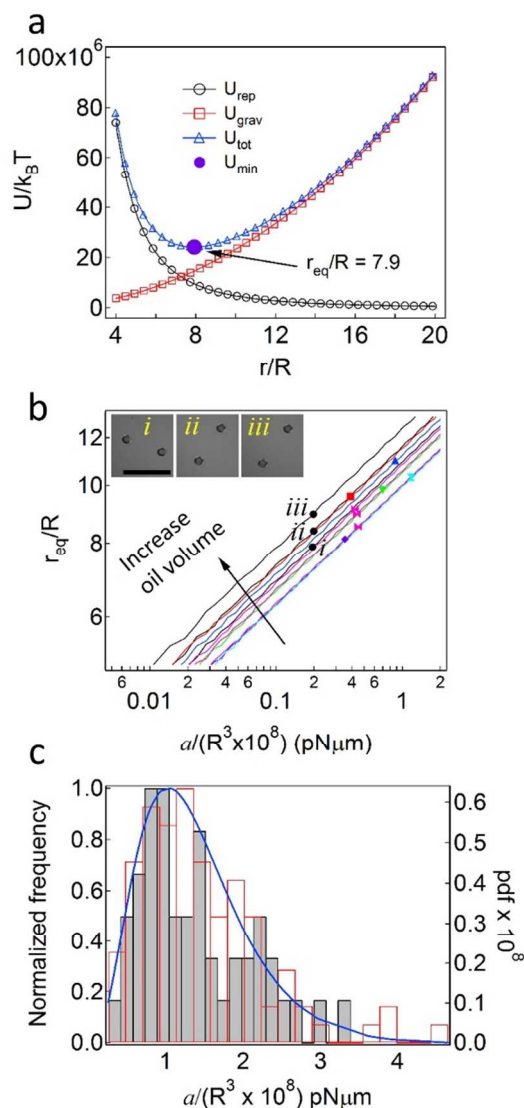


Fig. 3 Determination of the pair interaction magnitude. (a) Equilibrium separation determined by the energy minimization of the interaction potentials in which $a/(R^3 \times 10^8) = 0.2$ pN $\cdot\mu$ m and $V_{oil} = 53$ μ L are used in the calculations. (b) Examples of equilibrium separation as a function of the interaction magnitude and the oil volume. Symbols indicate experimental separation between two particles in which the same symbols represent the same particle pairs in a different amount of oil. The scale bar in the snapshots is 1 mm. (c) Histogram of heterogeneous pair interactions for 47 pairs at the curved oil-water interface.

Using the repulsive interaction and the gravitational potential, the total interaction potential between two particles at the curved oil-water interface ($U_{tot}(r) = U_{rep}(r) + U_{grav}(r)$) can be calculated as a function of particle separation for a constant value of a (the magnitude of repulsive interactions). As shown in Fig. 3a, the electrostatic repulsion (U_{rep}) decays as r^{-3} , whereas the potential energy (U_{grav}) monotonically increases with r due to gravity and geometrical confinement. By finding the minimum (U_{min}) in the total interaction potential, we can determine the corresponding equilibrium separation of r_{eq}/R . The same procedure is repeated by varying the values of a and V_{oil} , and the consequent equilibrium separations as a function of

a for different values of V_{oil} are shown in Fig. 3b. The magnitude of repulsive interactions (a) can be obtained by using the experimental value of the equilibrium separation for a given pair of particles in an oil lens of volume V_{oil} , as indicated by symbols in Fig. 3b.

We find that the experimentally determined values of the interaction magnitude (a) depend on particle pairs. As shown in Fig. 3c, the histogram of the repulsive interaction magnitudes measured over 47 particle pairs are significantly heterogeneous (grey bars), following a gamma distribution (the blue solid line is the probability density function, pdf)

$$f(a; k, \theta) = a^{k-1} \frac{e^{-a/\theta}}{\theta^k \Gamma(k)}, \quad (3)$$

where k and θ are the shape and scale parameters, respectively, and $\Gamma(k)$ is the gamma function. The fitted parameter values with 95% confidence intervals are $k = 3.85$ and $\theta/R^3 = 3.62 \times 10^7$ pN· μ m. Note that the experimentally obtained value of a for the same particle pair does not significantly change as V_{oil} increases, as indicated by the same symbols in Fig. 3b. In this case, the equilibrium separation increases with V_{oil} because the radius of curvature of the oil-water interface around the center region increases as V_{oil} increases (Fig. 2b), allowing the particles to move farther apart.

To investigate the effect of interaction heterogeneity on the structure of particle arrangements at the curved oil-water interface, we generate particle arrangements using MC simulations and use the experimentally determined pair potentials and heterogeneity as the input parameters. In the MC simulations, N particles at the interface repel each other due to the electrostatic repulsion

$$\frac{U_{rep,ij}}{k_B T} = \frac{a_{ij}}{r_{ij}^3} \quad (4)$$

where r_{ij} is the separation between i and j particles. Each particle in the N -particle configuration also experiences a gravitational potential, which can be expressed as

$$U_{grav} = g(\rho_p V_p - \rho_w V_{pw} - \rho_o V_{po})h(\lambda). \quad (5)$$

Assuming pairwise additivity,^{15, 35} the potential of an individual particle i , used in the MC simulations, consists of the sum of all pair interactions with its surrounding particles (j) and its gravitational energy as

$$U_i = U_{grav,i} + \sum_j^N U_{rep,ij} \quad (i \neq j). \quad (6)$$

The total energy of the N -particle configuration at the curved oil-water interface can then be expressed as: $U_{tot} = \sum_i^N U_i$ ($i \neq j$). To introduce the effect of the interaction heterogeneity in the MC simulation, we use the two experimentally determined scale and shape parameters to regenerate the gamma distribution for the N particles. It is assumed that i and j particles possess their own half-pair potential, $a_i = a_j = a_{ij}/2$,

and their sum corresponds to the magnitude of the pair interaction ($a_{ij} = a_i + a_j$) that is also consistent with the gamma distribution (red bars in Fig. 3).¹⁵ Interestingly, the measured pair interactions in this work are similar to our previous work in which the pair interactions between two polystyrene microparticles ($R \approx 1.5 \mu$ m) at the planar oil-water interface were measured by optical laser tweezers.¹⁵ The pair interaction results in the previous work were found to be heterogeneous following the gamma distribution with the similar value of the shape parameter of $k = 4.4$. The pair interaction heterogeneity at the interface may be attributed to non-uniform charge distribution,^{36, 37} but the further quantitative investigation should be required to understand the exact mechanism.

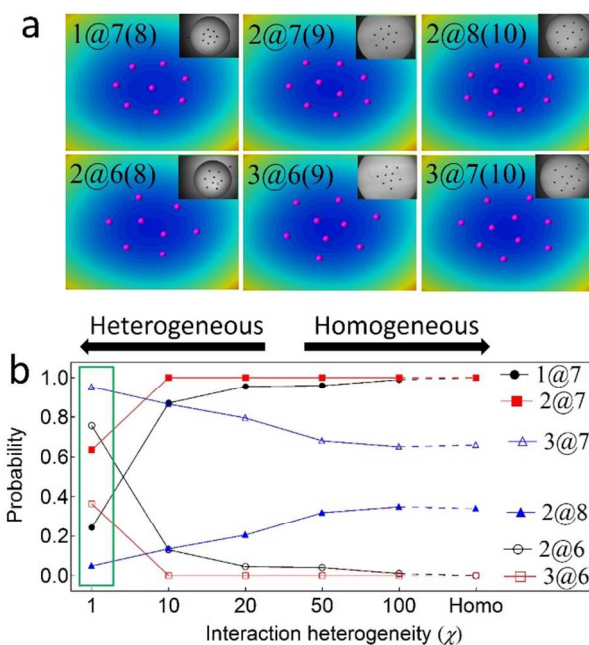


Fig. 4 Effect of the interaction heterogeneity on the arrangement behaviours. (a) Example arrangement structures obtained from MC simulations with introduced interaction heterogeneity. (b) Probability of each arrangement structure depending on the interaction heterogeneity obtained from the simulations. The green box indicates the probabilities when experimental heterogeneity is introduced to the simulations. 200 runs of MC simulations at a given χ value and a given particle number are executed.

The measured pair interaction heterogeneity is important because it can provide a clue for finding hierarchical relations between small scale properties and bulk scale behaviours of colloidal particles at fluid-fluid interfaces. Previously, we found that the radial distribution function (RDF) of 2D bulk suspensions of polystyrene microparticles is consistent with the RDF obtained from MC simulations when the interaction heterogeneity measured by the optical laser tweezers is introduced to the simulations.¹⁵ This previous result demonstrates that the microscale measurement (i.e., pair interactions) directly affects the large scale measurement (i.e., microstructure).

Similar to the previous work, the simulated configuration structures of eight, nine, and ten particles incorporating the interaction heterogeneity (Fig. 4a) are in excellent agreement with the experimental observations; that is, the particles form the two different structures that were experimentally observed in Fig. 1. We recognize two important factors that affect the arrangement behaviours at the curved interface: interaction heterogeneity and kinetics. For the cases of eight- and nine-particle configurations, we find that the simulations with a homogeneous potential of $a = \langle a_{ij} \rangle = k\theta/R^3 \approx 1.4 \times 10^8$ pN $\cdot\mu\text{m}$ (i.e., the mean value of a_{ij}) dominantly result in one type of arrangement structure, 1@7 and 2@7, respectively, suggesting that the presence of the two different structures in the experiments can be attributed to the effect of the interaction heterogeneity. For the ten-particle configurations, however, particles can organize into either structure, 2@8 or 3@7, even if the homogenous potential is used in the simulations (Fig. 4b). This simulation result for ten particles indicates that a kinetic factor also plays an important role in the arrangement behaviour. The relative contribution between the interaction heterogeneity and kinetics on the arrangement behaviour seems to depend on the degree of heterogeneity and the number of particles.

We further run MC simulations to quantify the effect of interaction heterogeneity. To vary the interaction heterogeneity, the shape and scale parameters for the experimental gamma distribution are multiplied and divided by a magnification factor (χ), $k\chi$ and θ/χ , such that the pair interaction becomes more homogeneous as the value of χ is increased while keeping the mean value of the interaction potential ($k\theta$) constant. As shown in Fig. 4b, we find that the frequency of the configurations that possesses the higher number of inner particles (2@6, 3@6, and 3@7) increases as the heterogeneity increases. For example, nine particles dominantly form 2@7 when the interactions are homogeneous, and the frequency of 3@6 increases upon increasing the heterogeneity. It is likely that, as the heterogeneity increases, the probability of the presence of particles with weaker half-pair potentials increases; these particles tend to segregate to the center of the arrangement structures. Indeed, from further analyses of the simulations of nine particles, we confirm that when the particles form the 3@6 structure, the three inner particles dominantly possess the three weakest half-pair potentials among all the nine particles in the arrangement structure. Similarly, the half-pair potentials of the inner particles in the 2@6 and 3@7 structures are found to be weaker than those of the outer particles. This simulation result is consistent with the calculation of the total energy (U_{tot}) of the arrangement structures in which the structure with a larger number of inner particles becomes energetically more favourable as the heterogeneity increases.

Conclusions

We have investigated the effect of interaction heterogeneity between particles on their arrangement behaviour at the curved

oil-water interface. Based on the energy minimization associated with the electrostatic repulsion between two particles and their gravitational potentials, we found that the magnitude of pair interactions is heterogeneous depending on the particle pairs. This interaction heterogeneity directly affects the arrangement configurations of the particles at the curved interface, leading to diversity in their structures. Based on MC simulations, we found that the particle structures can be controlled by varying the interaction heterogeneity. In general, the number of inner particles increases as the interaction heterogeneity increases, and the inner particles possess weaker half-pair potentials, compared to those of the outer particles at thermodynamic equilibrium. Furthermore, we found that the kinetic factor also plays an important role in the arrangement behaviour. The relative contribution between the interaction heterogeneity and the kinetics on the arrangement behaviours warrants future investigation.

We also notice that although the half-pair potential approach efficiently works in MC simulations, an important question can be raised at this point. In a real colloidal system, it is unknown how much each particle possesses its own potential that may be called an intrinsic potential. In other words, there are an infinitely large number of combinations that can satisfy the relation of $a_{ij} = a_i + a_j$ (e.g., $a_i = a_{ij}/2$ and $a_j = a_{ij}/2$; $a_i = a_{ij}/3$ and $a_j = 2a_{ij}/3$; $a_i = a_{ij}/4$ and $a_j = 3a_{ij}/4$; $a_i = 2a_{ij}/5$ and $a_j = 3a_{ij}/5$; ...). Determination of the intrinsic potential may be feasible by using the current experimental system. In order to measure the intrinsic potentials of three particles (a_1, a_2, a_3), for instance, three independent conditions should be required. One condition can be the pair interaction (a_{12}) between particle-1 and -2 in the presence of the two particles at the curved oil-water interface. Another condition can be found in the triangular structure of three particles ($\mathbf{r}_1, \mathbf{r}_2$, and \mathbf{r}_3) upon adding the third particle to the interface. The other condition should correspond to the energy minimum of the triangular structure (E_{min}). Consequently, the three unknown variables (a_1, a_2, a_3) can be solved by the three independent conditions. In this way, the intrinsic potentials of additional particles can be subsequently obtained by adding particles one after another. In short, the current experimental system and the analysing method can provide a route for determining such intrinsic potentials and potentially clarify the physical meaning of the intrinsic potentials of colloids trapped at fluid-fluid interfaces (e.g., dipole strength, surface charge, etc.).

Another interesting feature based on the simulation results is that the current experimental system can be used for sorting the large number of particles in the order of the intrinsic potentials. This condition can be achieved by subjecting sufficient energy (e.g., *via* vibration) to the system such that the particles at the curved interface adopt a thermodynamically stable configuration. The resulting equilibrium structure of the particles would correspond to a radially distributed structure in which the particles with lower intrinsic potentials collect on the center regions of the curved oil-water interface and the particles with higher intrinsic potentials occupy the surrounding regions of the interface. All things considered, we believe that this work

will prompt further fundamental studies such as investigating the transition dynamics of arrangement structures, the packing mechanism, and the packing geometry driven by the repulsive interaction at non-planar fluid-fluid interfaces.

Acknowledgements

B. J. Park acknowledges financial support from Basic Science Research Program through the National Research Foundation of Korea (NRF) funded by the Ministry of Science, ICT & Future Planning (NRF-2014R1A1A1005727). D. Lee acknowledges funding from the NSF CAREER Award (DMR-1055594) and the PENN MRSEC DMR11-20901 through the NSF.

Notes and references

^aDepartment of Chemical Engineering, Kyung Hee University, Yongin, 446-701, South Korea

^bDepartment of Chemical and Biomolecular Engineering, University of Pennsylvania, Philadelphia, Pennsylvania, 19104, United States

Corresponding authors: Bum Jun Park: (Tel) +82-31-201-5276, (email) bjpark@khu.ac.kr

- B. P. Binks and T. S. Horozov, *Colloidal Particles at Liquid Interfaces*, Cambridge University Press, New York, 2006.
- B. P. Binks, *Curr. Opin. Colloid Interface Sci.*, 2002, 7, 21-41.
- S. U. Pickering, *J. chem. Soc. Trans.*, 1907, 91, 2001-2021.
- W. Ramsden, *Proc. R. Soc. London*, 1903, 72, 156-164.
- D. Stamou, C. Duschl and D. Johannsmann, *Phys. Rev. E*, 2000, 62, 5263-5272.
- P. A. Kralchevsky and K. Nagayama, *Langmuir*, 1994, 10, 23-36.
- M. Oettel and S. Dietrich, *Langmuir*, 2008, 24, 1425.
- P. Pieranski, *Phys. Rev. Lett.*, 1980, 45, 569-572.
- A. J. Hurd, *J. Phys. A: Math. Gen.*, 1985, 45, L1055-L1060.
- R. Aveyard, B. P. Binks, J. H. Clint, P. D. I. Fletcher, T. S. Horozov, B. Neumann, V. N. Paunov, J. Annesley, S. W. Botchway, D. Nees, A. W. Parker, A. D. Ward and A. N. Burgess, *Phys. Rev. Lett.*, 2002, 88, 246102-246104.
- B. J. Park and E. M. Furst, *Soft Matter*, 2011, 7, 7676-7682.
- B. J. Park, J. P. Pantina, E. M. Furst, M. Oettel, S. Reynaert and J. Vermant, *Langmuir*, 2008, 24, 1686-1694.
- C. L. Wirth, E. M. Furst and J. Vermant, *Langmuir*, 2014, 30, 2670-2675.
- K. Masschaele, B. J. Park, E. M. Furst, J. Fransaer and J. Vermant, *Phys. Rev. Lett.*, 2010, 105, 048303.
- B. J. Park, J. Vermant and E. M. Furst, *Soft Matter*, 2010, 6, 5327-5333.
- L. Botto, E. P. Lewandowski, M. Cavallaro and K. J. Stebe, *Soft Matter*, 2012, 8, 9957-9971.
- L. Botto, L. Yao, R. L. Leheny and K. J. Stebe, *Soft Matter*, 2012, 8, 4971-4979.
- T. Brugarolas, B. J. Park and D. Lee, *Adv. Funct. Mater.*, 2011, 21, 3924-3931.
- K. D. Danov, P. A. Kralchevsky, B. N. Naydenov and G. Brenn, *J. Colloid Interface Sci.*, 2005, 287, 121-134.
- A. Dominguez, M. Oettel and S. Dietrich, *J. Phys.: Condens. Matter*, 2005, 17, S3387-S3392.
- E. P. Lewandowski, J. A. Bernate, P. C. Searson and K. J. Stebe, *Langmuir*, 2008, 24, 9302-9307.
- E. P. Lewandowski, M. Cavallaro, L. Botto, J. C. Bernate, V. Garbin and K. J. Stebe, *Langmuir*, 2010, 26, 15142-15154.
- E. P. Lewandowski, P. C. Searson and K. J. Stebe, *J. Phys. Chem. B*, 2006, 110, 4283-4290.
- J. C. Loudet, A. M. Alsayed, J. Zhang and A. G. Yodh, *Phys. Rev. Lett.*, 2005, 94, 018301-018304.
- R. Aveyard, J. H. Clint, D. Nees and V. N. Paunov, *Langmuir*, 2000, 16, 1969-1979.
- B. Madivala, J. Fransaer and J. Vermant, *Langmuir*, 2009, 25, 2718-2728.
- J.-Y. Wang, Y. Wang, S. S. Sheiko, D. E. Betts and J. M. DeSimone, *J. Am. Chem. Soc.*, 2011, 134, 5801-5806.
- M. Cavallaro, L. Botto, E. P. Lewandowski, M. Wang and K. J. Stebe, *Proc. Natl. Acad. Sci. U.S.A.*, 2011, 108, 20923-20928.
- M. E. Leunissen, A. Van Blaaderen, A. D. Hollingsworth, M. T. Sullivan and P. M. Chaikin, *Proc. Natl. Acad. Sci. U.S.A.*, 2007, 104, 2585-2590.
- W. T. Irvine, V. Vitelli and P. M. Chaikin, *Nature*, 2010, 468, 947-951.
- Y. Lin, H. Skaff, T. Emrick, A. D. Dinsmore and T. P. Russell, *Science*, 2003, 299, 226-229.
- B. J. Park and D. Lee, *Langmuir*, 2013, 29, 9662-9667.
- J. Burton, F. Huisman, P. Alison, D. Rogerson and P. Taborek, *Langmuir*, 2010, 26, 15316.
- V. N. Paunov, *Langmuir*, 2003, 19, 7970-7976.
- B. J. Park, B. Lee and T. Yu, *Soft Matter*, 2014, DOI: 10.1039/C1034SM01823K.
- J. D. Feick, N. Chukwumah, A. E. Noel and D. Velegol, *Langmuir*, 2004, 20, 3090-3095.
- S. Tan, R. L. Sherman, D. Qin and W. T. Ford, *Langmuir*, 2004, 21, 43-49.

Table of contents entry

Interaction heterogeneity affects the particle arrangements at the curved oil-water interface, leading to diversity in the arrangement structures.

